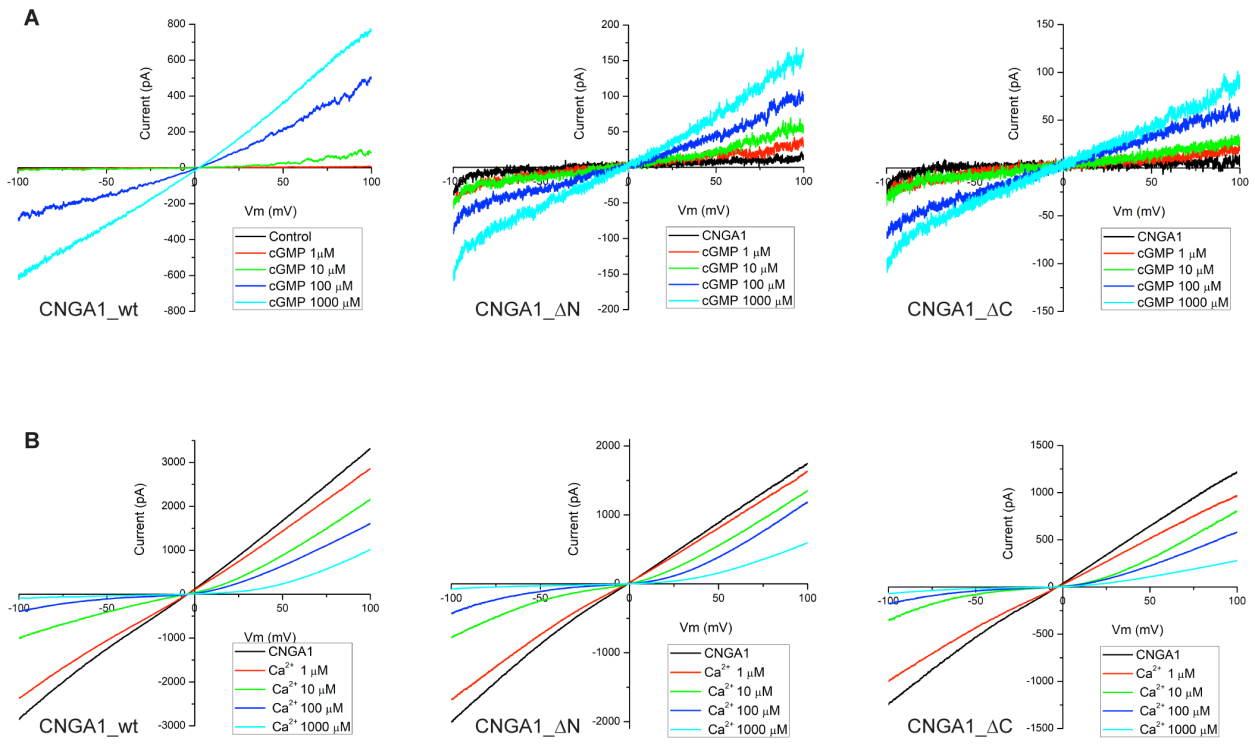

Figure S1. Intracellular cGMP activation and extracellular Ca^{2+} blockage of human CNGA1 and its truncation mutants, Related to Figure 1

(A) Sample I-V curves of human CNGA1 and its truncation mutants recorded in excised patches with varying cGMP concentrations in the bath (cytosolic). Currents at 100 mV were used to generate the concentration dependent cGMP activation curve shown in Figure 1A.

(B) Sample I-V curves of human CNGA1 and its truncation mutants recorded using patch clamp in whole-cell configuration with varying Ca^{2+} concentrations in the bath (extracellular). The pipette solution contains 1 mM cGMP. Currents at -100 mV were used to generate the concentration dependent Ca^{2+} inhibition curve shown in Figure 1B.

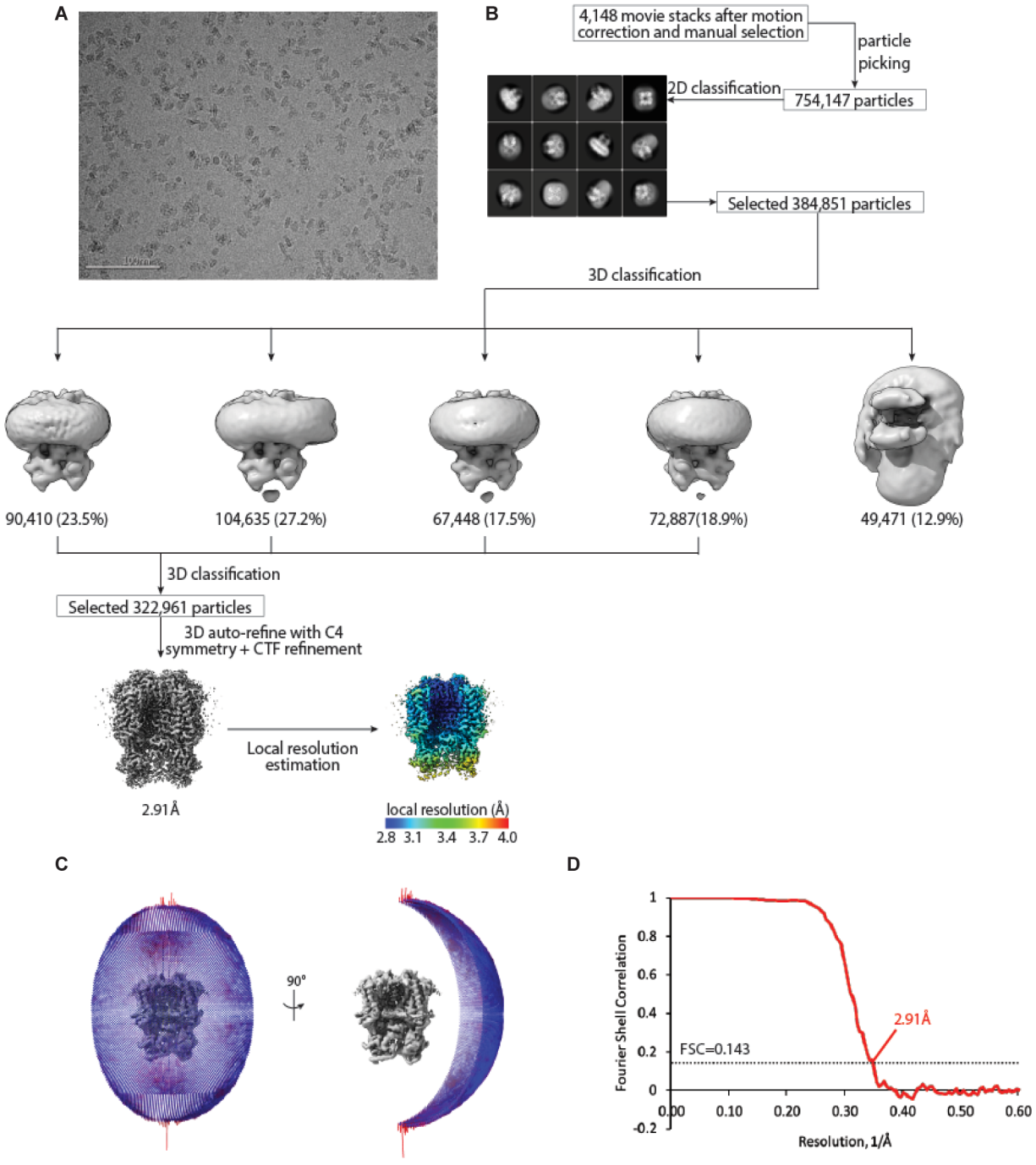

Figure S2. Cryo-EM data processing scheme of the cGMP-bound human CNGA1, Related to Figure 1 and STAR Methods

(A) A representative micrograph. Scale bar is at 100 nm.

(B) Flow chart of the cryo-EM data processing procedure. Selected 2D class averages are shown. The particle numbers are indicated under the corresponding 3D classes with the percentage of the selected particles after 2D classification in parentheses for the first round of 3D classification.

(C) Euler angle distribution of particles used in the final three-dimensional reconstruction.

(D) Fourier Shell Correlation curves showing the overall resolution of 2.91 Å at FSC=0.143.

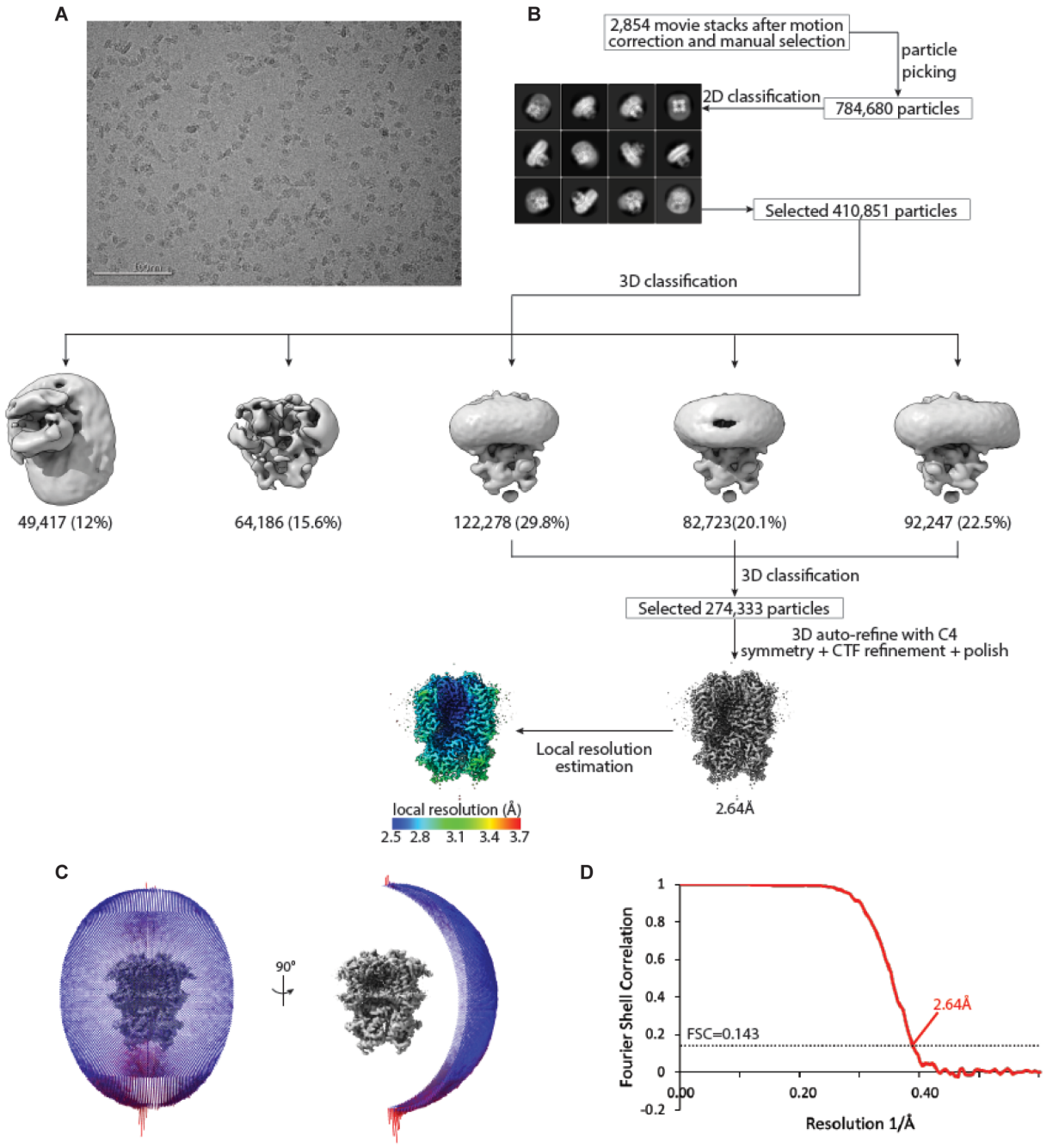

Figure S3. Cryo-EM data processing scheme of the apo closed human CNGA1, Related to Figure 1 and STAR Methods

(A) A representative micrograph. Scale bar is at 100 nm.

(B) Flow chart of the cryo-EM data processing procedure. Selected 2D class averages are shown. The particle numbers are indicated under the corresponding 3D classes with the percentage of the selected particles after 2D classification in parentheses for the first round of 3D classification.

(C) Euler angle distribution of particles used in the final three-dimensional reconstruction.

(D) Fourier Shell Correlation curves showing the overall resolution of 2.64 Å at FSC=0.143.

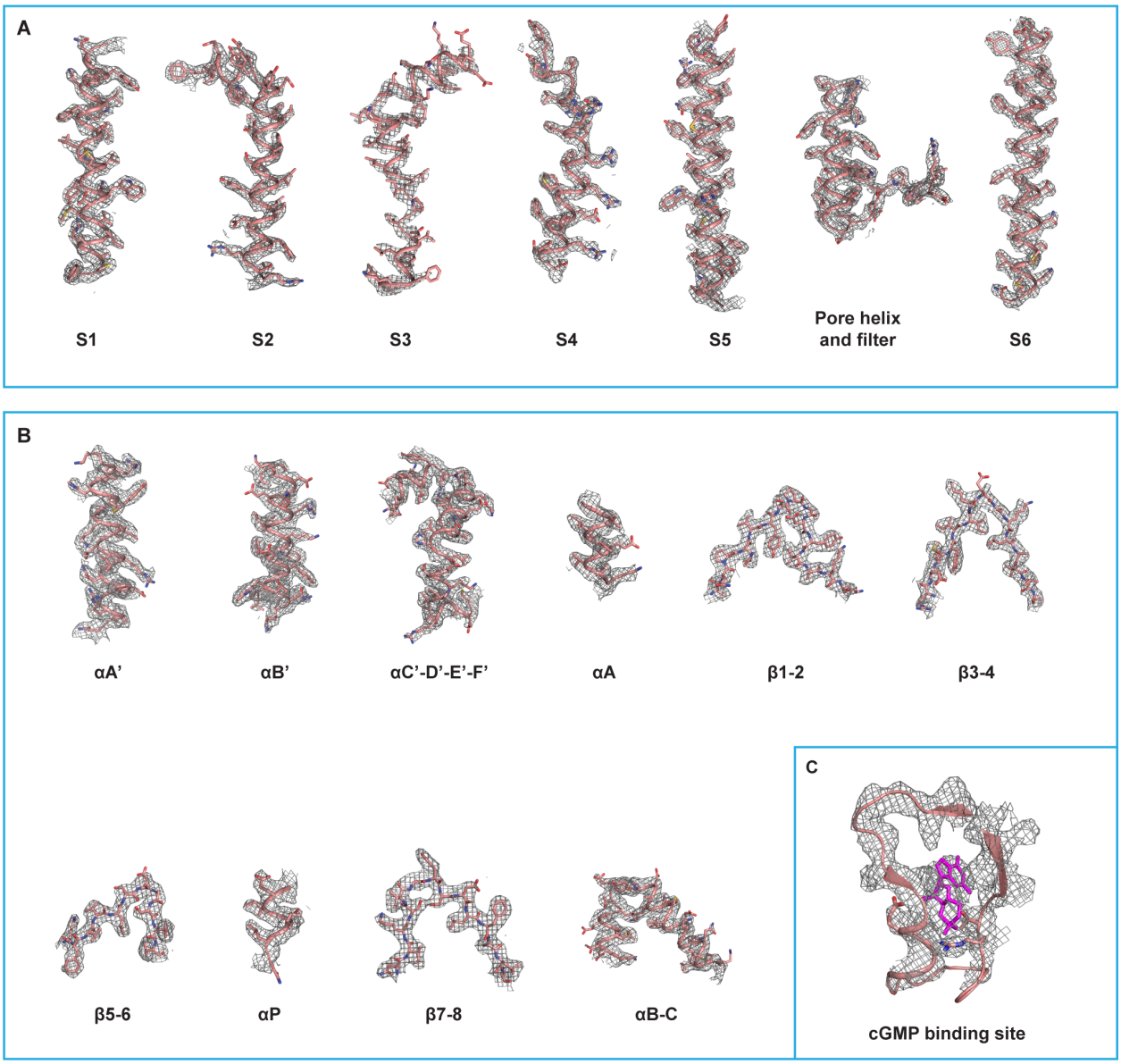

Figure S4. Sample density maps of human CNGA1, Related to Figure 1
(A) Maps of the transmembrane region from the apo CNGA1 structure contoured at 7 σ. The transmembrane region of CNGA1 has higher local resolution than the cytosolic soluble region.
(B) Maps of the cytosolic region from the apo CNGA1 structure contoured at 4 σ.
(C) Density map of cGMP-binding pocket in the open CNGA1 structure contoured at 5 σ. cGMP is shown in purple stick.

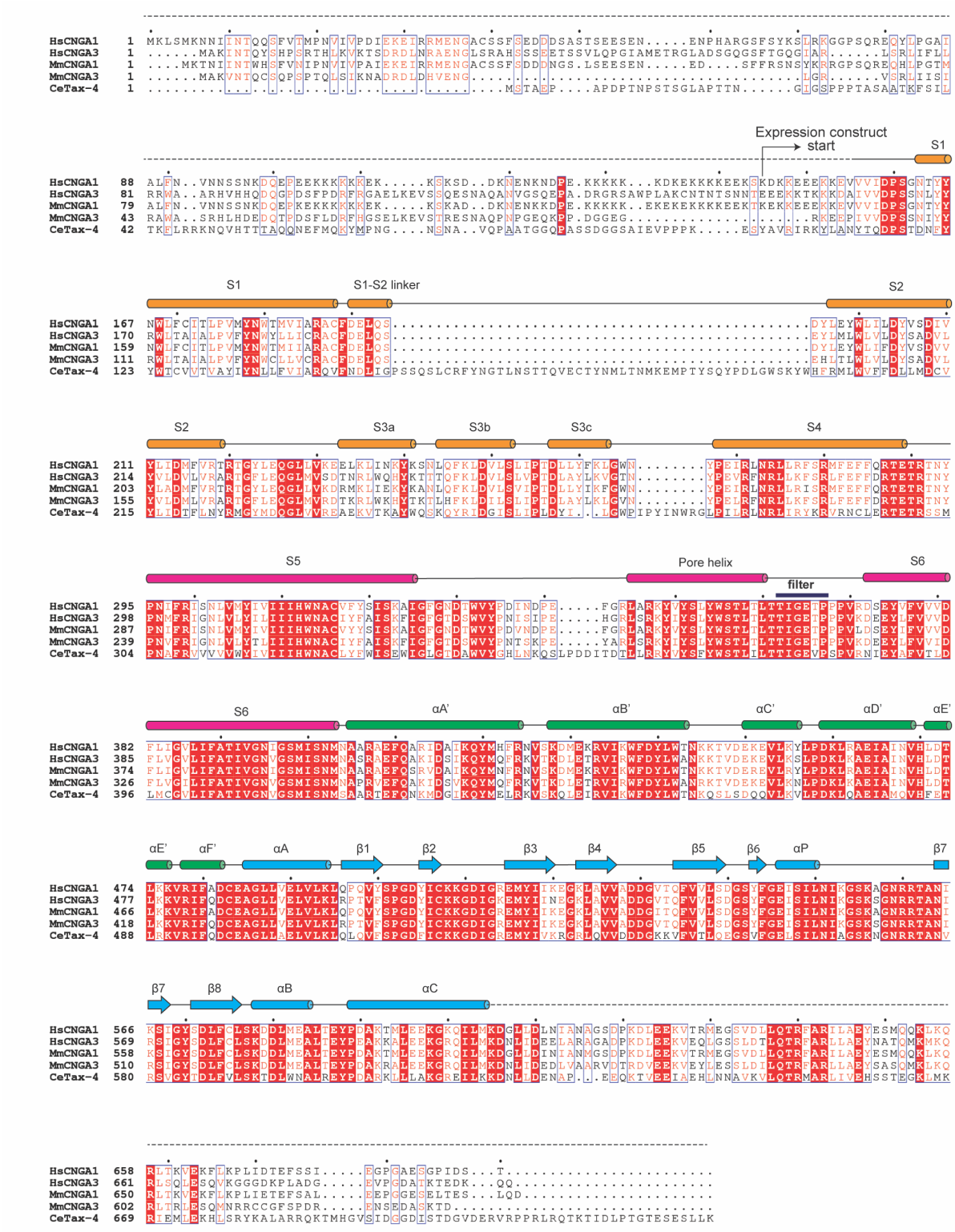

Figure S5. Multiple sequence alignment of CNG, Related to Figure 1
Sequence alignment of human CNGA1 and A3, mouse CNGA1 and A3, and *C. elegans* TAX-4. Secondary structure assignments are based on the structure of apo human CNGA1.

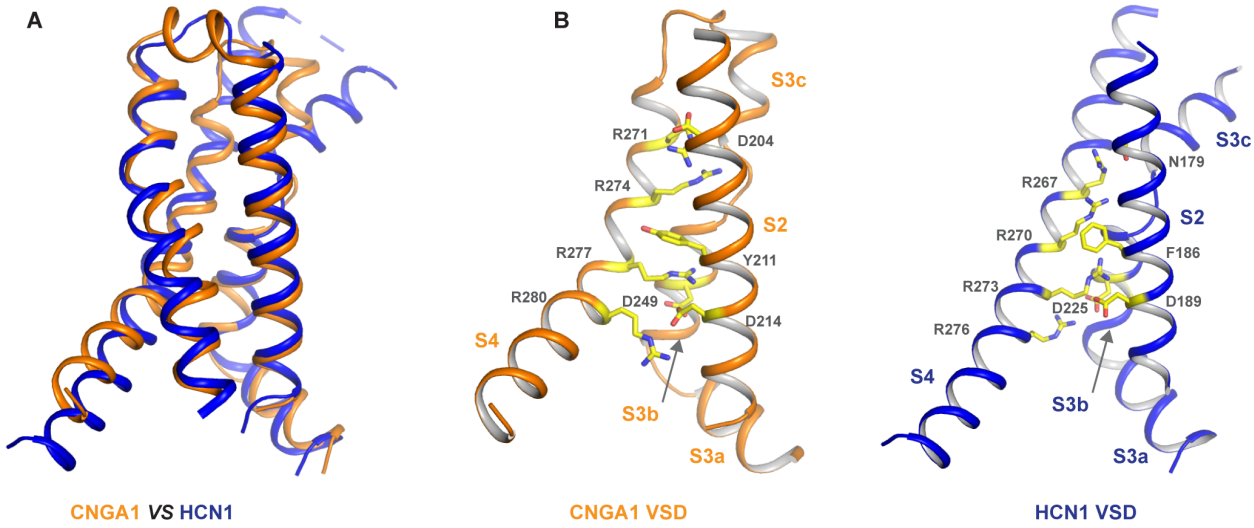

Figure S6. Structural comparison of VSD between human CNGA1 and HCN1, Related to Figure 1

(A) Overall structural alignment of VSD from the apo CNGA1 structure (brown) and VSD of human HCN1 in depolarized state (blue, PDB code: 5U6P)

(B) Side-by-side comparison between CNGA1 VSD and HCN1 VSD with some key residues conserved in canonical voltage sensor shown. S1 helices are omitted in both structures for clarity.

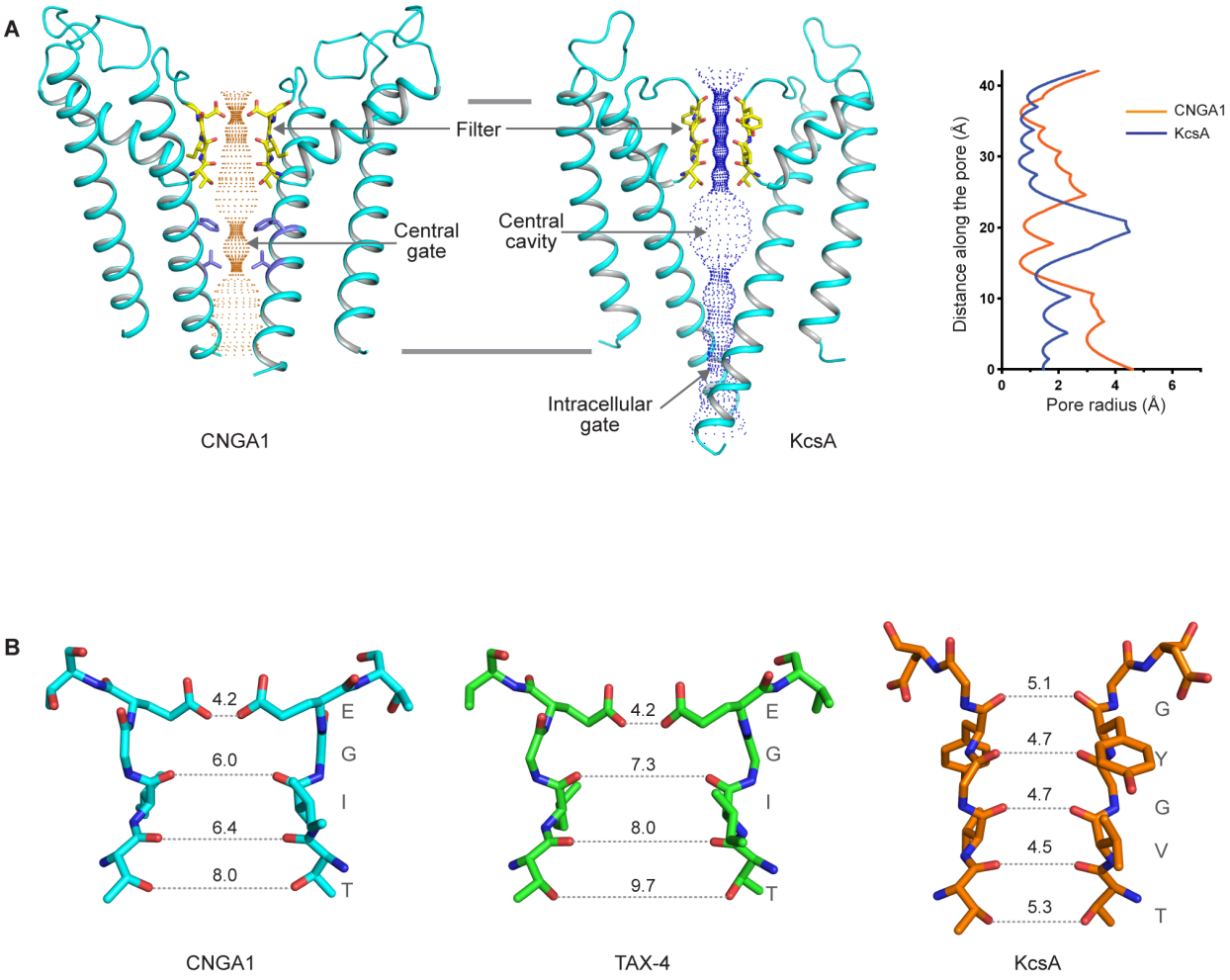

Figure S7. Comparison of ion conduction pore between human CNGA1 and K^+ channel, Related to Figure 2

(A) Structural comparison of the closed ion conduction pore between CNGA1 and KcsA K^+ channel (PDB code:1K4C) with front and rear subunits removed for clarity. Ion pathway is marked with dotted mesh.

(B) Comparison of the filter dimension between CNGA1, TAX-4 (PDB code:6WEJ), and KcsA.

	Apo CNGA1 in K^+/Ca^{2+} (EMDB-23306, PDB-7LFT)	**cGMP-bound CNGA1 in K^+/Ca^{2+}** (EMDB-23307, PDB-7LFW)	**cGMP-bound CNGA1 in Na^+/Ca^{2+}** (EMDB-23308, PDB-7LFX)	**cGMP-bound CNGA1 in Na^+** (EMDB-23309, PDB-7LFY	**cGMP-bound CNGA1_E365Q in Na^+/Ca^{2+}** (EMDB-23310, PDB-7LG1)
Data collection and processing					
Magnification	81,000	81,000	105,000	105,000	105,000
Voltage (kV)	300	300	300	300	300
Electron exposure (e–/Å^2)	60	60	60	60	60
Defocus range (μm)	-0.9 - -2.2	-0.9 - -2.2	-0.9 - -2.2	-0.9 - -2.2	-0.9 - -2.2
Pixel size (Å)	0.844	0.839	0.805	0.829	0.817
Symmetry imposed	C4	C4	C4	C4	C4
Initial particle images (no.)	784,680	754,147	644,905	523,867	890,458
Final particle images (no.)	274,333	322,961	76,571	73,011	311,051
Map resolution (Å)	2.64	2.91	3.05	3.56	2.67
FSC threshold	0.143	0.143	0.143	0.143	0.143
Refinement					
Initial model used (PDB code)	5H3O	5H3O	5H3O	5H3O	5H3O
Model resolution (Å)	2.64	2.91	3.05	3.56	2.67
FSC threshold	0.143	0.143	0.143	0.143	0.143
Map sharpening *B* factor (Å^2)	-88	-135.9	-120.7	-150.2	-89.6
Model composition					
Non-hydrogen atoms	15479	14846	14846	14851	15017
Protein residues	1800	1800	1800	1800	1800
Water	4	0	0	4	4
Ligands (cGMP/Ion)	0/3	4/2	4/2	4/3	4/1
Lipid	32	0	0	0	0
B factors (Å^2)					
Protein	40.58	49.97	49.97	49.97	49.30
Ligand	32.98	86.07	86.07	85.44	86.63
R.m.s. deviations					
Bond lengths (Å)	0.009	0.005	0.005	0.005	0.005
Bond angles (°)	1.098	0.896	0.897	0.897	0.923
Validation					
MolProbity score	1.56	1.59	1.58	1.60	1.62
Clashscore	8.59	9.72	9.55	9.82	11.03
Poor rotamers (%)	0.25	0.25	0.25	0.25	0.24
Ramachandran plot					
Favored (%)	97.54	97.66	97.71	97.66	97.77
Allowed (%)	2.46	2.34	2.29	2.34	2.23
Disallowed (%)	0	0	0	0	0

Table S1. Cryo-EM data collection and model statistics, Related to Figure 1 and STAR Methods

Lipid molecules were modeled in the apo closed CNGA1 structure only. The structure of cGMP-bound CNGA1 in K^+/Ca^{2+} was directly fit into the EM maps of cGMP-bound CNGA1 in Na^+ and in Na^+/Ca^{2+} without further refinement.